Journal of Materials Chemistry

PAPER

Molecular conformation dependent emission behaviour (blue, red and white light emissions) of all-*trans*-β-carotene-ZnS quantum dot hybrid nanostructures†

V. Perumal Devarajan,[a] Devaraj Nataraj,*[abd] Thangavelu Pazhanivel,[ab] Karuppanan Senthil,[c] Minsu Seol,[d] Kijung Yong,[d] Justus Hermannsdorfer[e] and Rhett Kempe[e]

A novel hybrid material consisting of all-*trans*-β-carotene and ZnS quantum dots (QDs) was prepared by two different controlled experiments and their photophysical properties were investigated in detail. Depending upon the preparation method, the β-carotene molecule had formed either an upright or wrapped conformation around the ZnS QDs and consequently the interaction between these two hybridizing systems was either charge transfer induced or electrostatic in type, respectively. Optical absorption, Raman and FTIR investigations have confirmed the two different conformations of the molecule around the ZnS QDs. Because of the two different conformations and the consequent interactions, different emission colours, such as blue and red wavelengths were obtained from these hybrids. We were also able to obtain white light emission by using cadmium doped ZnS QDs for the hybrid preparation.

1. Introduction

Research on organic–inorganic hybrid materials is gaining wide spread importance because of their superior properties make them suitable for various applications.[1,2] Organic molecules such as polymers or bio-molecules are hybridized with inorganic quantum nanostructures to produce new physical and chemical properties. The electron affinity and band gap values of two hybridizing materials can be chosen in such a way that a desired band alignment (either type-I or type-II) is developed between them. Further by tuning the size of the inorganic material, which is usually nanoscale in size, one can also fine tune the relative energy level separation between two hybridizing materials. Depending upon the band alignment and the relative energy level separation between two hybridizing materials, different applications are possible. For example, if the interface between two hybridizing materials is type-I, with a high offset, then photogenerated electron–hole pairs are confined well in the core nanostructure, thus giving an enhanced emission yield.[3,4] On the other hand if the interface is type-II, one carrier is confined in the core nanostructure, whereas the other is transferred to the shell material.[5,6] Thiol capped CdTe QDs are a good example of a material with enhanced emission yield.[7] There the relative energy levels between the CdTe QDs and various thiol groups of molecules is such that photoexcited holes were not trapped by the molecule and therefore an enhanced emission yield was noticed. When the same group of thiol molecules were used to cap CdSe QDs then the relative energy levels between them are such that the molecular level has favoured hole trapping and therefore the emission yield from CdSe QD was quenched. Inorganic–organic heterostructures such as Sb_2S_3–P3HT,[8] CdS–P3HT,[9] carbon nanotube–P3HT[10] are some of the combinations studied for solar energy conversion applications. Here the band alignment is type-II in nature and therefore photogenerated electron–hole pairs are separated, upon light illumination.

In general organic–inorganic hybrids do not require lattice matching, because the organic counterpart is an amorphous substance. Relative energy level position between the two hybridizing substances and their respective band gap energies only determine the nature of interface, whether it is type I or type II. Further, organic molecules, including bio-molecules, try to establish contact with the inorganic nanostructures through weak short range forces, such as van der Waals and electrostatic type interactions, or otherwise form chemical bonds through their functional groups.[11–13] Therefore it is because of these flexibilities, various combinations of inorganic–organic materials is possible,

[a] *Thin Films & Nanomaterials Research Laboratory, Department of Physics, Bharathiar University, Coimbatore-641 046, India. E-mail: de. natraj2011@gmail.com; Fax: +91-422-2422387; Tel: +91-422-2428444*

[b] *DRDO-BU CLS, Bharathiar University Campus, Coimbatore-641 046, India*

[c] *School of Advanced Materials Science & Engineering, Sungkyunkwan University (Suwon Campus), Cheoncheon-Dong 300, Jangan-gu, Suwon 440-746, South Korea*

[d] *Surface Chemistry Laboratory of Electronic Materials, Department of Chemical Engineering, Pohang University of Science and Technology (POSTECH), Pohang 790-784, Republic of Korea*

[e] *Inorganic Chemistry II, University of Bayreuth, 95440 Bayreuth, Germany*

† Electronic supplementary information (ESI) available. See DOI: 10.1039/c2jm32982d

but, understanding the resulting hybrid material's photophysical and other properties becomes a real challenging. It has also been reported that the nature of conformation of the molecule around the quantum nanostructure can influence the functional properties. For example, if the molecule is wrapped around the QD's surface then higher FRET efficiency is possible.[14] Bio-molecules such as DNA have shown different conformations around nanostructures and therefore have resulted in different functional behaviours.[15–17] It is because of all these interesting properties and challenges that hybrids have gained a wide spread importance among scientists around the world. As an result there are several reports on the preparation, characterization and application of hybrids. They include peptide–inorganic based hybrids for bio-sensing applications,[18] graphene–polyaniline based hybrid materials for super capacitors,[19] zeolite L-polymer hybrids with luminescence properties[20] and CNT–organic hybrids for gas sensing applications.[21]

In the present work, we have used the natural molecule all-*trans*-β-carotene to cover the surface of ZnS QDs and investigated the resulting hybrid structures photophysical properties. All-*trans*-β-carotene is a well known linear conjugated molecule and its structure has a backbone of eleven carbon double bonds as shown in Fig. 1. This molecule can readily form a charge transfer complex with iodine and HNO_3 molecules and therefore its natural absorption is photobleached.[22] There are several reports on the investigation of β-carotene, and which are mostly fundamental in nature.[23–26] Recently, this molecule was successfully introduced into carbon nanotube nanostructures and investigated for its structural stability and conformation.[27] However, studies on the hybrids of β-carotene are limited and therefore the nature of interaction between β-carotene and quantum nanostructures, like QDs, nanowires, and nanotubes has not been explored. Similarly the wide band gap semiconductor ZnS QD is a nanostructure well known for its luminescence properties. There are several reports on the preparation, characterization and application of ZnS QDs.[28–30] ZnS QDs can give strong luminescence at around 420–440 nm and which is due to deep lying sulfur vacancy states resulting from a deviation in the stoichiometry.[31–33] In the absence of sulphur vacancy states, a strong excitonic emission is resulted as reported elsewhere.[34] Further, depending upon dopant atom, the emission colour from ZnS QD is tuneable as well. For example if doped with Mn^{2+} ions, in the place of Zn^{2+}, then the excited ZnS lattice can transfer its energy to the Mn^{2+} ions and consequently an orange emission is obtained at 590 nm.[35] If cadmium ions are doped into the crystal lattice of ZnS then a green emission is obtained.[36,37]

Here, in our present work we have hybridized these two potential materials by two different methods and investigated their photophysical properties in detail.
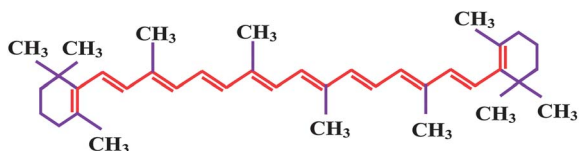

Fig. 1 Structure of all-*trans*-β-carotene.

2. Materials and methods

Chemicals and reagents

Zinc chloride ($ZnCl_2$, ≥98%, Sigma), sodium sulfide (Na_2S, Fulka), β-carotene Type-I (β-c, ≥93% (UV), Sigma), ethanol (Eth, absolute 99.9%, Sigma-Aldrich) and double distilled water (DD water) have been used to prepare the quantum dots and hybrid system.

Instruments

X-ray diffraction patterns (XRD) and high-resolution transmission electron microscope (HR-TEM) images were obtained from the as prepared ZnS QDs and their hybrids, to determine the structure and morphology of the samples, respectively. The PANalytical diffractometer (model: X' Pert PRO) with Cu K_α radiation of wavelength 0.1542 nm was used for the X-ray diffraction studies. The diffraction data were collected over the 2θ range of 10 to 100° in steps of 0.05°, while the tube voltage and current were 40 kV and 30 mA, respectively. The surface morphology images were recorded using either JEOL-300 model HRTEM or TEM Zeiss Libra 200 FE instruments. Elemental analysis was also conducted using an EDAX facility attached with HR-TEM. A UV-visible spectrophotometer (model: Shimatzu 3600) was used for the optical absorption measurements. Raman and FTIR spectra were also recorded from these samples to determine the nature of hybridization between the ZnS QD and β-carotene. Raman spectra were recorded using a JASCO (model: NRS-3100) Raman spectrometer with a 532 nm laser source and FTIR spectra were recorded using a SENSIR FTIR spectrometer (model: illuminatIR). Room temperature excitation and emission spectra were recorded from a Horiba Jobin Yvon spectrofluorometer (model: FLUOROMAX-4) with a 450 W Xenon source.

Chemical method of hybrid formation

At first 0.01 mole zinc chloride ($ZnCl_2$) solution was prepared by dissolving the same in double distilled water (DD water) and keeping the as prepared solution under ultrasonic agitation, at room temperature. β-carotene solution (0.001 mole dissolved in ethanol) was then added drop wise. To this mixture solution an equimolar solution (0.01 mole dissolved in DD water) of freshly prepared sodium sulfide (Na_2S) was added drop wise to obtain the ZnS QD, β-carotene hybrid sample. The as obtained product is a colloidal suspension, which was washed in DD water several times to remove any un-reacted or excess precursor molecules. After washing several times, the dispersed particles were centrifuged at 10 000 rpm for 10 min, so that a red coloured gel like hybrid sample was obtained. This gel like substance was then subjected to drying under a rotary vacuum condition for a few days, so that a powdery substance was obtained. This final powder was then subject for further characterization.

Physical or direct mixing method of hybrid formation

A 0.01 mole $ZnCl_2$ solution was prepared by dissolving the same in DD water and keeping the as prepared solution under ultrasonic agitation, at room temperature, an equimolar solution (0.01 dissolved in DD water) of freshly prepared Na_2S was then

added drop wise to obtain ZnS QDs. The obtained product is a colloidal suspension, which was washed several times in DD water to remove any un-reacted or excess precursor molecules. After washing, the sample was centrifuged at 10 000 rpm for 10 minutes and then naturally dried to get ZnS QD powder. The as obtained ZnS QD powder sample was then mixed with β-carotene solution (dissolved in ethanol) directly. The resulting colloidal solution was dried naturally for a few days and then the as obtained powder sample was characterized for its structural and photophysical properties.

3.   Results and discussion

Structure and optical properties

Fig. 2 shows the X-ray diffraction patterns of (a) pure ZnS QDs and (b) the ZnS/β-carotene hybrid sample prepared by the chemical method. All the observed diffraction peaks, in both samples, are similar and also matching with the standard cubic zinc blend structure of the ZnS crystal system (JCPDS 05-566). By using the Debye–Scherer formula, we have calculated the average particle size[38] and which is about 5 nm in both samples. The calculated lattice parameter value for ZnS QDs is 0.5415 nm and which agrees with the standard lattice parameter value of the
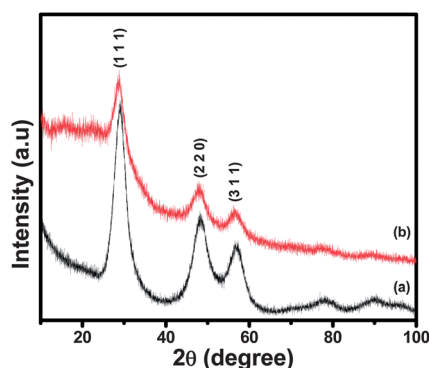

Fig. 2 XRD patterns of (a) pure ZnS QDs and (b) ZnS/β-carotene hybrid system prepared by the chemical method.

cubic ZnS crystal lattice. The HR-TEM investigation on the ZnS QDs samples showed the size distribution and shape details of the QDs (Fig. 3a). The size is about 6 nm and it is spherical in morphology. A similar HR-TEM investigation on the chemically prepared hybrid sample showed a clustered morphology as shown in Fig. 3b and c. The buried presence ZnS QDs in the molecular network of β-carotene, is the reason for this clustered morphology. Elemental mapping corresponding to this clustered morphology shown in Fig. 3c indicated the presence of elements like zinc (d), sulphur (e) and carbon (f) in this sample (Fig. 3(d–f)). The zinc and sulphur are from the ZnS QDs, whereas the carbon is from the β-carotene. From the composition analysis it was found that both the ZnS QDs and ZnS QD/β-carotene hybrid sample (chemical) are stoichiometric in nature and their respective composition values are $Zn_{46}S_{54}$ and $Zn_{48}S_{52}$ (see Fig. S1 in ESI† for EDAX spectra). XRD and HR-TEM investigations were also conducted on the directly mixed hybrid sample. The XRD pattern from this hybrid sample is similar to that of pure ZnS QDs. The HR-TEM images also showed a cluster like morphology, similar to that obtained from the chemically prepared hybrid sample (figures are not shown).

Fig. 4 shows the optical absorption spectra of (a) pure ZnS QDs and (b) its hybrid sample prepared by the chemical method. The ZnS QDs showed a blue shifted absorption maximum at 280 nm and this is due to the quantum confinement effect in the nanoparticles. The hybrid sample (chemical) also showed a similar absorption spectrum with a maximum at 290 nm. We do not seen β-carotene's absorption band in this hybrid sample and this is possible only if charge transfer complex is formed between these two hybridizing systems. Here β-carotene is interacting with the QD surface and therefore a charge transfer interaction is possible between these two systems. The optical absorption spectrum was also recorded from the directly mixed hybrid sample and it is given in Fig. 4 (curve c). In the directly mixed sample we saw absorption bands from both the ZnS QDs and β-carotene, respectively, at 280 nm and 450 nm. The presence of β-carotene's absorption band indicates that charge transfer complex formation is not favoured in the hybrid sample prepared by the direct mixing method. For comparison purposes, the
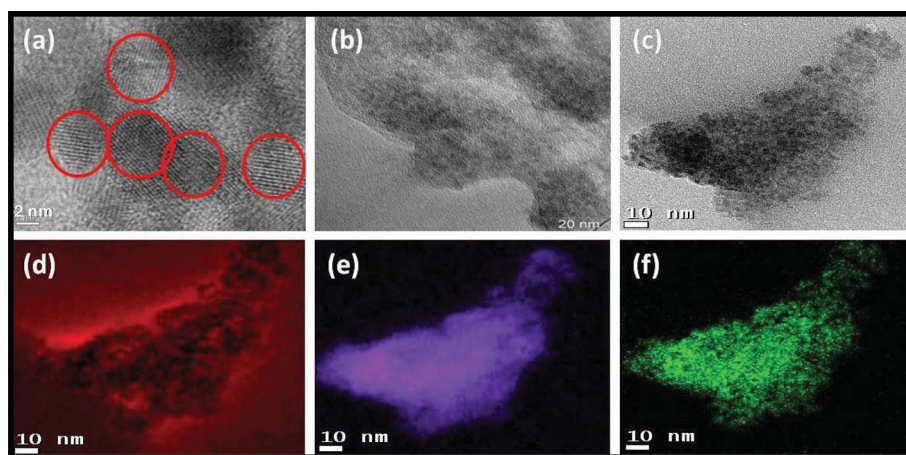

Fig. 3 HR-TEM images of (a) pure ZnS QDs. (b) and (c) Cluster like morphology of ZnS/β-carotene hybrid system prepared by the chemical method. (d), (e) and (f) Elemental mapping corresponding cluster morphology in (c). Carbon (d), Zinc (e) and sulphur (f) distributions are shown. The background red colour in (d) is from the carbon grid.
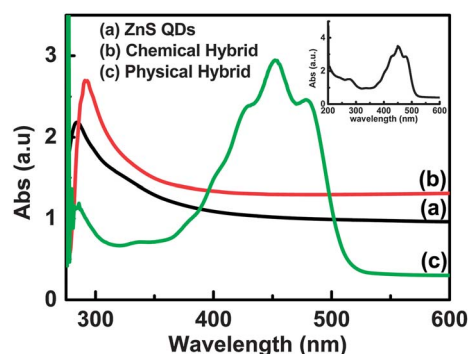
Fig. 4 Absorption spectra of (a) pure ZnS QDs; (b) ZnS/β-carotene hybrid system prepared by the chemical method and (c) ZnS/β-carotene hybrid system prepared by the physical method. Inset of this figure is optical absorption spectrum of pure carotene.

optical absorption spectrum of pure β-carotene is also given in the inset of Fig. 4 and it shows a visible band in the range 350 to 525 nm, with a maximum at 450 nm. Note that this molecule's absorption spectrum also shows a weak band at around 280 nm, and as it is indistinguishable from the absorption band of ZnS QDs at 280 nm, they are merged in the directly prepared sample.

Raman analysis

To confirm the outcome of optical absorption data, Raman analysis was carried out on these hybrid samples. The Raman spectrum recorded from the chemically prepared hybrid sample is shown in Fig. 5(b). For comparison purposes, the Raman spectrum from pure β-carotene is also given in Fig. 5(a). Pure β-carotene has nine carbon double bonds (C=C) and which together form an average stretching vibrational mode at 1522 cm^{-1} (v_1 mode). In addition to this v_1 mode, there are two other modes at about 1154 (v_2 mode) and 1006 cm^{-1} (v_3 mode). The v_2 mode is due to the mixed vibrations of C=C, C–C stretching and CH in plane vibrations of β-carotene. The v_3 mode is due to C–CH$_3$ stretching vibration between the main chain of the β-carotene and the side methyl groups attached with it. The frequency positions of the observed vibrational modes match the reported values of pure β-carotene.[39] In the case of the chemically

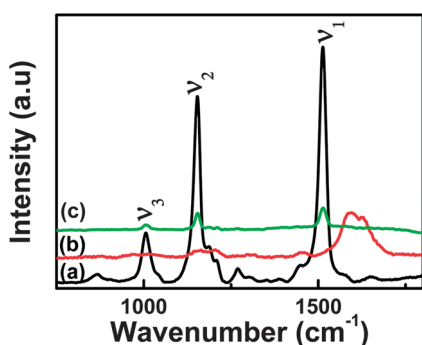**Fig. 5** (A) Raman spectra of (a) pure β-carotene (b) the ZnS/β-carotene hybrid system prepared by the chemical method; (c) the ZnS/β-carotene hybrid system prepared by the direct mixing method. (Spectrum (b) and (c) are Y-axis shifted for better understanding).

prepared hybrid sample, the v_1 mode is blue shifted and its intensity has been reduced as well. The observed blue shift indicates that this vibrational mode is stiffened because of the charge transfer induced interaction with ZnS QDs. The Raman shifts usually confirm the charge transfer induced interaction between two hybridizing materials and therefore has been widely used. For example, when carbon nanostructures like carbon nanotubes[40] and graphene[41] interact with some organic molecules, then a charge transfer type interaction is developed between these two systems and this can be determined by observing the shift in the Raman vibrational modes of either the carbon nanostructure or the interacting molecule. Expansion or contraction of the lattice results, respectively, due to the transfer of electrons or holes into the nanostructure.[40] Here the interacting counterpart is an organic molecule and therefore either an expansion or contraction of bond length is possible, respectively, due to the transfer of electrons or holes into the molecule. As the molecule has established a charge transfer induced interaction with the QD by transferring its electrons to the QD's surface, holes are produced in the molecule and consequently a stiffening effect in the molecule results because of the bond length contraction. Interestingly similar analysis on the directly prepared hybrid sample does not show any Raman shift (Fig. 5c) and this means that there is no charge transfer induced interaction between these two hybridizing systems, when directly mixed. The Raman results have thus supported the optical absorption data from these hybrids.

Photoluminescence properties

Emission from the chemically prepared sample. To determine the emission behaviour from these hybrid samples we have recorded their photoluminescence spectra, by exciting the samples at their respective optical absorption maximum or excitation energy. Pure ZnS QDs showed an excitonic UV emission band at 330 nm, as shown in Fig. 6A. The sulphur vacancy assisted blue emission band is weak in our as prepared pure ZnS QDs and this is because of the stoichiometry of the system.[34] In the case of the chemically prepared ZnS/β-carotene hybrid sample (excited at 280 nm), a broad blue emission band was obtained as shown Fig. 6B. This spectrum was curve fitted and which led to five emission bands centred at (a) 330, (b) 370, (c) 420, (d) 470 and (e) 540 nm. The 330 nm emission band from ZnS QDs is excitonic in type. The 370 nm emission band could be due to interstitial zinc (I_{Zn}), as reported elsewhere.[42] The emission band at 420 nm is a sulphur vacancy (V_S) assisted one, caused by the transition from the 'V_S' state to the valence band edge state of ZnS QDs. All of these observed radiative transitions are schematically represented in the energy band diagram (Fig. 7). Apart from these defect related emission bands, we have also noticed an unusual blue emission band at 475 nm which is red shifted from the other defect related emission bands of ZnS QDs. We believe that this emission band is due to interfacial related transitions between β-carotene and ZnS QDs. The photoexcited ZnS QD's conduction band electrons can make a radiative transition to the highest occupied molecular orbital (HOMO) level of β-carotene and recombine with the holes in that energy level (Fig. 7). We have calculated (see ESI† for calculation details) the energy level separation between the conduction band
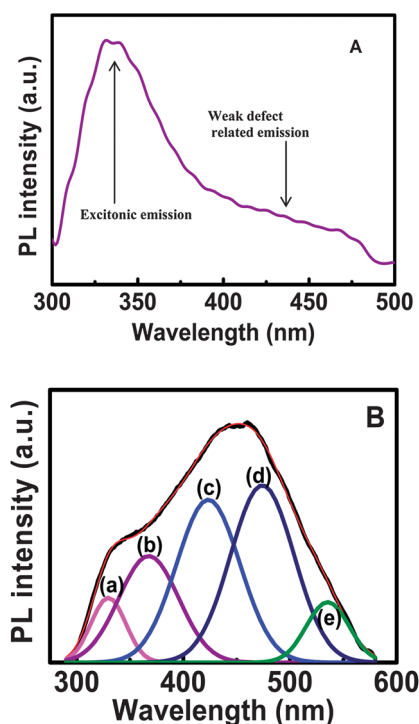
Fig. 6 Emission spectrum of (A) pure ZnS QDs. The strong excitonic emission band is represented by the up arrow and the weak defect related blue emission band is represented by the down arrow; (B) ZnS/β-carotene hybrid system prepared by the chemical method. Deconvoluted spectra are also given in this figure and the red line is due to Gaussian curve fittings (an explanation of the deconvoluted emission spectra are given in the text).

edge state of ZnS QDs and the HOMO level of β-carotene as 2.57 eV and which closely matches the experimental emission wavelength at 2.61 eV (475 nm).
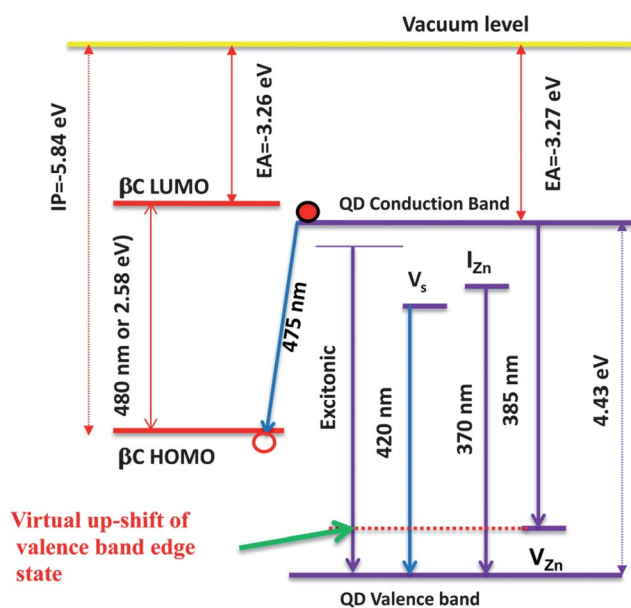

Fig. 7 Schematic interfacial energy band diagram between β-carotene and ZnS QDs; virtual up-shift of the valence band edge state is pointed to by the green arrow.

In addition to this emission band at 475 nm we have also noticed a weak defect related emission band at 540 nm as shown in Fig. 6B which is similar to the band observed in the literature, and accordingly it is assigned to some self-activated centers, probably surface states, vacancy or interstitial states within the structure.[43,44]

Emission from the directly mixed hybrid sample. Fig. 8A shows the emission spectrum from the directly mixed ZnS/β-carotene hybrid sample and it shows both 'UV' and 'red' emission bands at 350 nm and 600 nm, respectively, from the ZnS QDs and β-carotene. The UV band is an excitonic type emission from ZnS QDs. The red emission band is from β-carotene.[45] The relative intensity of the UV emission band is very weak and this observation is not clear. In order to understand the reason for this observation we have recorded the individual emission spectrum from ZnS QDs and β-carotene. Pure ZnS QDs give out an excitonic emission band (curve (a) in Fig. 8B), as has already been discussed in the chemically prepared sample part. β-Carotene has given out its natural red emission (curve (b) in Fig. 8B). When both of them are mixed together, then the resulting emission spectrum shows emission features of the ZnS QDs and β-carotene in the 'UV' and 'red' regions, respectively (curve (c) in Fig. 8B). An interesting observation is that the emission intensity
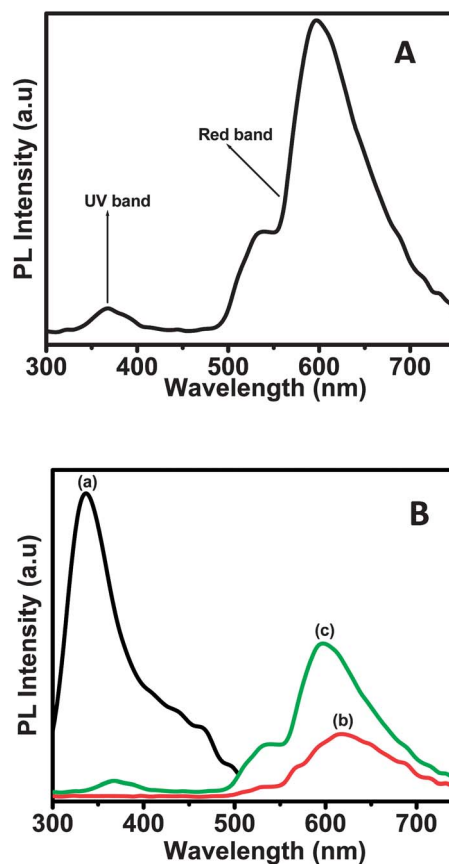

Fig. 8 (A) Emission spectrum from the directly prepared ZnS/β-carotene hybrid sample at an excitation energy of 280 nm; (B) emission spectra of (a) pure ZnS QDs (b) pure β-carotene and (c) the ZnS/β-carotene mixture solution (Ex: 280 nm).

from the ZnS QDs was drastically decreased, whereas the emission intensity from the β-carotene was increased. We therefore believe that there is an energy transfer type interaction between the ZnS QDs and β-carotene molecules. The critical requirement for an energy transfer induced interaction is satisfied in this directly prepared hybrid sample. That is, the emission spectrum of donor ZnS QDs (weak blue emission bands) overlaps with the absorption maximum of β-carotene (blue absorption bands) and therefore an energy transfer induced interaction[46] is possible between these two systems, as has been observed in other QD/bio-molecule hybrids.[47,48]

Hybrid formation

Although the crystal structure, morphology and chemical composition details of the hybrid samples, prepared by the two different methods, are similar, the optical absorption, Raman and photoluminescence results have shown entirely different characteristics. As the linear molecule can easily undergo conformational change around the QDs, as was reported for other linear molecules, we believe that β-carotene can also undergo a similar conformational change around the ZnS QDs, and become responsible for the observed differences in the photophysical properties. The fundamental difference between the two preparation methods could be the reason for two different conformations. In the case of the chemical preparation method, we have added β-carotene just before the addition of Na_2S and therefore the molecule can establish a weak local binding with the precursor ($ZnCl_2$) molecule through a charge transfer process, in a similar manner as between carotene and HNO_3.[22] An optical absorption measurement of the mixture solution of β-carotene and $ZnCl_2$ also confirmed the charge transfer type interaction between them, by showing a weak band at around 1000 nm (see Fig. S2 in the ESI†). We have added Na_2S into this mixture solution (β-carotene-$ZnCl_2$), so that ZnS QD formation has started occurring in the solution, and it was

evident from the optical absorption spectrum itself, which has shown an increase in the optical absorption value, in particularly in the UV region of the spectrum (see Fig. S2 in ESI†). It has to be noted that we did not see a charge transfer complex band at 1000 nm, in the case of the ZnS QD–carotene hybrid sample prepared by the chemical method, which was obtained after the complete experimental procedure (see Fig. S2 in the ESI†). Though initially the molecule had established a charge transfer complex with $ZnCl_2$, once the ZnS QDs had formed, then naturally the molecule started interacting with the ZnS QD surface. HR-TEM images from the hybrid samples clearly show the presence of ZnS QDs buried in the carotene molecular network. Therefore, based on these experimental observations we come to the conclusion that a micelle like structure is formed at first as shown in Fig. 9A. When Na_2S is introduced the growth of the ZnS QDs starts at the center of the micelle. In the resulting hybrid, the molecule has an upright conformation with its length is being perpendicular to the QD surface as shown in Fig. 9A. As the defect states due to surface distributed positive ions and their vacancies of ZnS QDs (at a depth of 385 nm, from the conduction band edge state) are in a favourable position to receive electrons from the HOMO level of β-carotene (Fig. 7), a charge transfer complex is now formed between β-carotene and the ZnS QDs, in this conformation. The photobleached optical absorption band of β-carotene and the Raman shifts from this chemically prepared hybrid are the direct evidence for this charge transfer type interaction. Further, it is because of these transferred charges (from carotene to ZnS QD's defect level at 385 nm) and its population (the population is due to the larger surface to volume ratio of the QD) the valence band edge level of the ZnS QDs is virtually up shifted. Upon light illumination, these trapped charges are promoted from this virtual valence band edge state to the conduction band edge state of the ZnS QDs and therefore the difference between these two energy levels results in the excitation energy spectrum (see Fig. S3 in ESI†). It has to be noted further that, because these traps are occupied or
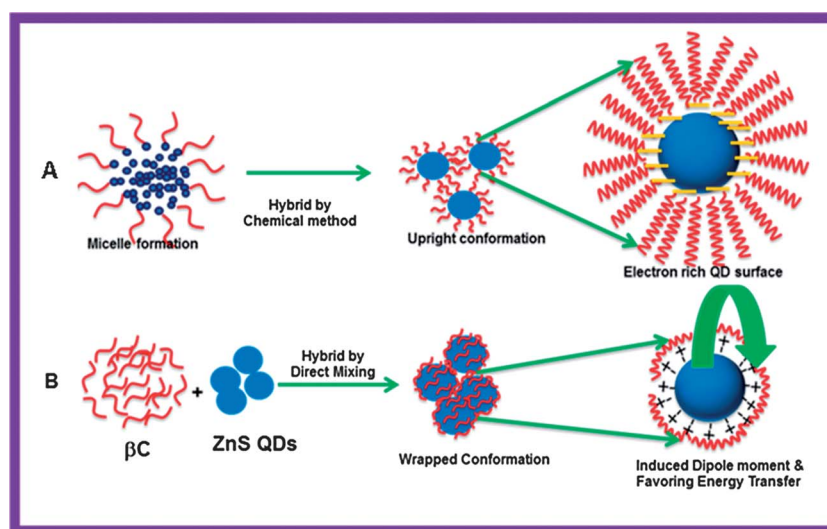

Fig. 9 Two different formation mechanisms of the hybrids and the resulting molecular conformation around the ZnS QDs. (A) Hybrid formation due to the chemical method and the up-right conformation of β-carotene around the ZnS QDs; (B) hybrid formation by the direct mixing method and the wrapped conformation of β-carotene around the ZnS QDs. The electron rich QD surface and induced dipole moments, respectively, corresponding to the upright and wrapped conformations are shown in this schematic diagram. Energy transfer interaction is represented by a curved green color arrow.

filled with electrons from carotene, the highest occupied molecular orbital energy (HOMO) level of carotene is looking for electrons. Therefore, excited electron transition from the conduction band edge state of the QD to this HOMO level of the molecule gives out a radiative emission at 475 nm, as was seen before.

In the case of the direct mixing method, we have used as prepared ZnS QDs, which are free from surface ligands and therefore their surface has many active sites to interact with the incoming molecules. Once the molecule is introduced then its entire length can develop local contact with the ZnS QD surface (wrapped conformation) by just displacing its carbon double bond electrons towards the surface distributed charges of the QD. Because of this displacement of electrons, an equal amount of positive charge is induced in the polyene chain of the molecule. Now the force of attraction in this 'charges separated state' is electrostatic type in nature. With this wrapped conformation, the molecule is not donating charges to QD and consequently its optical absorption band is not photobleached. Also its Raman active vibrational modes are not shifted. Fig. 9B schematically represents the hybrid formation process, in the case of the directly mixed sample, which eventually resulted in a wrapped conformation of the molecule around the ZnS QDs. It has been reported that "part of β-carotene" has developed local contact with bulk CdS by sharing its carbon double bond electrons and consequently the molecule has underwent a structural transformation from *trans* to *cis* isomerisation.[49] They confirmed this structural transformation through Raman analysis by observing some strong new vibrational modes from β-carotene at 1245 or 1138 cm^{-1}.[50,51] Here we have not seen any similar structural transformation. That is, we have not seen any new Raman peaks from this hybrid sample. In our case, because of larger surface to volume ratio of the QDs, there are more surface active sites and therefore the molecule's entire length can establish contact with the QD surface, and as a result any such structural transformation (*trans* to *cis*) is restricted in this ZnS QD–β-carotene hybrid system. It is because of this wrapped conformation around the ZnS QDs, and the induced dipole moment between these two interacting systems, energy transferred interaction is maximized here in this (directly prepared) hybrid sample, and consequently the β-carotene molecule has started emitting its characteristics emission with improved intensity.

FTIR analysis

To confirm the electrostatic type interaction between the molecule and QD, the FTIR spectrum was recorded from the directly mixed hybrid sample. The as recorded FTIR spectrum shows a strong absorption band at 1120 cm^{-1} as shown in Fig. 10(a) and this is similar to the one obtained from the β-carotene radical cation at 1151 cm^{-1}. Based on a previous report, we attribute this IR band to an induced dipole moment in the molecule.[52] In the case of the chemically prepared hybrid sample, the FTIR spectrum showed a weak band at 1116 cm^{-1} as shown in Fig. 10(b). The molecule's length is perpendicular to the QD surface and therefore the relative strength of the dipole moment (due to the local binding of the molecule with the QD surface) is weak in this hybrid sample and consequently this results in a weak band. For
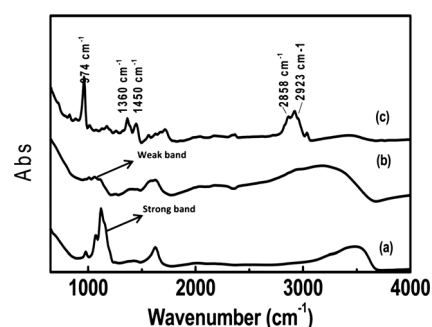

Fig. 10 FTIR spectrum of the (a) directly prepared (b) chemically prepared ZnS/β-carotene hybrid sample and (c) pure β-carotene.

comparison purpose pure β-carotene's FTIR spectrum is also given in Fig. 10(c). Pure β-carotene shows its characteristics vibrational modes, such as asymmetric and symmetric stretching vibrations of CH_2 and CH_3 at 2923 cm^{-1} and 2858 cm^{-1}, respectively. The other observed modes are a –CH=CH– out of plane deformation mode at 974 cm^{-1}, a CH_2 scissoring mode at 1450 cm^{-1} and a splitting due to the dimethyl mode at 1360 cm^{-1}.[53] Other vibrational modes are not visible in the presence of ZnS QDs and therefore were not seen in either of the hybrid samples.
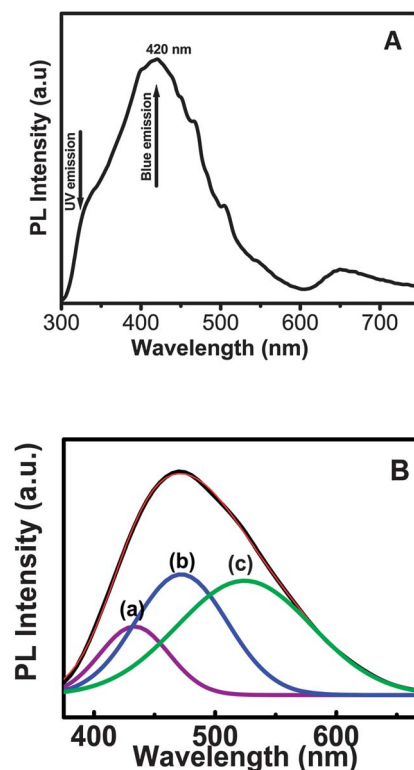

Fig. 11 Emission spectrum of (A) pure ZnS:Cd QDs at an excitation energy of 290 nm. The weak excitonic emission band is represented by the down arrow and the defect related blue emission is represented by the up arrow; (B) broad white emission from ZnS:Cd/β-carotene at an excitation energy of 350 nm from the chemically prepared hybrid sample. The deconvoluted spectra are also given in this figure and the red line represents Gaussian curve fitting.
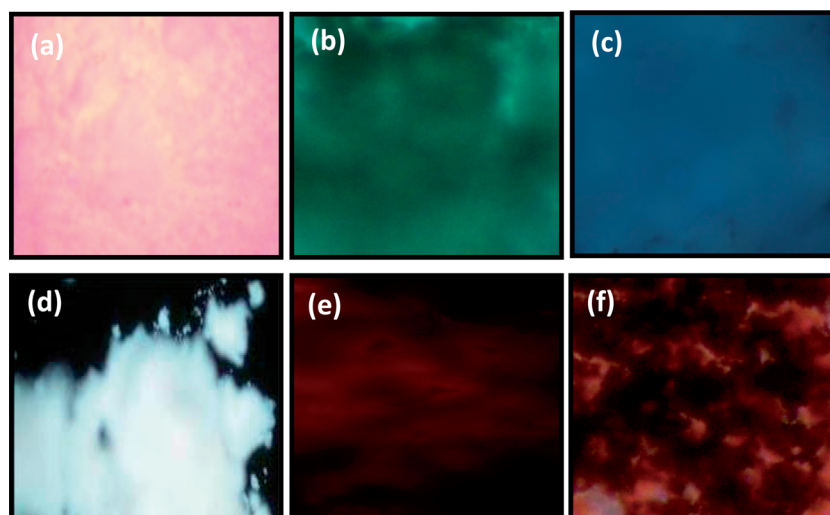
Fig. 12 Fluorescence microscope images of (a) pure ZnS QDs, (b) the ZnS/β-carotene hybrid sample by the chemical method, (c) pure ZnS:Cd QDs, (d) the ZnS:Cd/β-carotene hybrid sample by the chemical method, (e) the ZnS:Cd/β-carotene hybrid sample by the direct mixing method and (f) pure β-carotene.

ZnS:Cd–β-carotene hybrids

We have also extended similar experiments on cadmium doped ZnS QDs and its hybrids (see Fig. S4 in the ESI† for the XRD, HR-TEM data and preparation details). Depending upon the preparation method, whether it is chemical or physical methods, either 'charge transfer' or 'dipole moment induced electrostatic interaction' was established between the molecule and QD. A weak excitonic and defect related blue emission band was obtained from the Cd doped ZnS QDs sample (Fig. 11A). The defect related blue emission is strong in this sample because of the deviation in the stoichiometry of ZnS. The chemically prepared hybrid sample showed (excited at 350 nm) a broad emission band as shown in Fig. 11B and its deconvolution has resulted with three emission bands. The emission bands at (a) 435 nm and (b) 472 nm are due to sulphur vacancy assisted and interfacial related, respectively. The other broad emission band at 520 nm (curve (c)) is due to a Cd ion related green emission band. The entire emission band from this sample reassembled a white light spectrum, and we confirmed this by recording the white light emission from this sample under a fluorescence microscope (image (d) in Fig. 12). It has to be pointed out that getting white emission from a QD is an interesting research topic and there are several reports describing white light emitting behaviour from QDs, such as magic sized CdSe QDs,[54] trap rich CdS QDs[55] and alloyed $Zn_xCd_{1-x}Se$ QDs.[56] In all of the above systems, surface states determine the emission properties and, as it is difficult to control the trap state distribution, it also becomes difficult to see white light emission. But here we report a novel hybrid sample that shows white light emission which depends on both defect related and interface emissions.

In the case of the directly mixed sample (ZnS:Cd QDs with β-carotene), an enhanced red emission was seen from the β-carotene and this trend is exactly similar to that of the ZnS/β-carotene hybrid sample from the direct mixing method. We therefore reconfirmed the molecular conformation dependent emission behaviours of these Cd doped ZnS QD hybrid samples as well.

Optical microscope fluorescence images

To cross check the emission colours from the as prepared samples we have illuminated them under a UV fluorescence microscope and recorded the emission colours. For pure ZnS QDs, a purple colour was recorded. On the other hand for the chemically prepared ZnS hybrid, a pale green was obtained. In the case of Cd doped ZnS QDs, a blue emission was obtained. In the case of chemically prepared ZnS:Cd QDs/β-carotene hybrids, white emission was obtained. In all of the directly mixed samples, we noticed red emission, because of the energy transfer induced interaction between the β-carotene and QD. The as recorded emission colours are given in Fig. 12.

4. Conclusions

In conclusion, we have prepared inorganic–organic hybrid nanostructures of ZnS QD/β-carotene by two different methods and investigated their emission properties. In the case of chemically prepared hybrid sample, β-carotene is photobleached because of the charge transfer induced interaction with the ZnS QDs. Further we have noticed an interface related emission from this chemically prepared hybrid nanostructure and as result a broad blue emission was seen. In the case of the ZnS:Cd/β-carotene hybrid prepared by the chemical method, a white light emission was obtained. However, in the case of directly mixed hybrid sample the molecule and QD interacted differently; there was no charge transfer induced interaction between them, instead the molecule established a dipole moment induced weak electrostatic type interaction with the surface of the ZnS QDs. Because of this dipole moment induced interaction, and as well as the spectral overlap between the two hybridizing materials, the photoexcited ZnS QD transferred its energy to the β-carotene, thus resulting in an enhanced red emission from β-carotene. Based on the experimental results and photoluminescence behaviours, two different conformations were proposed for β-carotene around the ZnS QD. In the case of the chemically

prepared hybrid sample, an upright conformation was responsible for its photophysical behaviour. On the other hand, in the case of the physically mixed hybrids, a wrapped conformation is responsible for the resulting photophysical properties. We are planning to extend this work to other quantum nanostructures, to see new emission colours for application as biological image probes.

Acknowledgements

References

1 C. Sanchez, P. Belleville, M. Popall and L. Nicole, *Chem. Soc. Rev.*, 2011, **40**, 696–753.
2 J. M. Oh, D. H. Park and J. H. Choy, *Chem. Soc. Rev.*, 2011, **40**, 583–595.
3 P. Reiss, J. Bleuse and A. Pron, *Nano Lett.*, 2002, **2**, 781–784.
4 M. A. Hines and P. G. Sionnest, *J. Phys. Chem.*, 1996, **100**, 468–471.
5 S. A. Ivanov, J. Nanda, A. Piryatinski, M. Achermann, L. P. Balet, I. V. Bezel, P. O. Anikeeva, S. Tretiak and V. I. Klimov, *J. Phys. Chem. B*, 2004, **108**, 10625–10630.
6 D. Oron, M. Kazes and U. Banin, *Phys. Rev. B: Condens. Matter Mater. Phys.*, 2007, **75**, 035330.
7 S. F. Wuister, C. D. M. Donega and A. Meijerink, *J. Phys. Chem. B*, 2004, **108**, 17393–17397.
8 J. A. Chang, J. H. Rhee, S. H. Im, Y. H. Lee, H. J. Kim, S. I. Seok, Md. K. Nazeeruddin and M. Gratzel, *Nano Lett.*, 2010, **10**, 2609–2612.
9 S. Ren, L. Y. Chang, S. K. Lim, J. Zhao, M. Smith, N. Zhao, V. Bulovic, M. Bawendi and S. Gradecak, *Nano Lett.*, 2011, **11**, 3998–4002.
10 M. Bernardi, M. Giulianini and J. C. Grossman, *ACS Nano*, 2010, **4**, 6599–6606.
11 C. Sanchez, B. Julian, P. Belleville and M. Popall, *J. Mater. Chem.*, 2005, **15**, 3559–3592.
12 R. A. Sperling and W. J. Parak, *Philos. Trans. R. Soc. London, Ser. A*, 2010, **368**, 1333–1383.
13 I. L. Medintz, H. T. Uyeda, E. R. Goldman and H. Mattoussi, *Nat. Mater.*, 2005, **4**, 435–446.
14 W. R. Algar, M. B. Prigozhin, B. Liu, U. J. Krull and C. C. Gradinaru, *Proc. SPIE*, 2009, **7386**, 73860J.
15 S. Pu, A. Zinchenko and S. Murata, *Nanotechnology*, 2011, **22**, 375604.
16 W. J. Parak, T. Pellegrino, C. M. Micheel, D. Gerion, S. C. Williams and A. P. Alivisatos, *Nano Lett.*, 2003, **3**, 33–36.
17 W. R. Algar and U. J. Krull, *Langmuir*, 2006, **22**, 11346–11352.
18 D. Aili and M. M. Stevens, *Chem. Soc. Rev.*, 2010, **39**, 3358–3370.
19 H. Wang, Q. Hao, X. Yang, L. Lu and X. Wang, *Nanoscale*, 2010, **2**, 2164–2170.
20 H. Li, Y. Ding, P. Cao, H. Liu and Y. Zheng, *J. Mater. Chem.*, 2012, **22**, 4056–4059.
21 Y. Wang, N. Hu, Z. Zhou, D. Xu, Z. Wang, Z. Yang, H. Wei, E. S. W. Kong and Y. Zhang, *J. Mater. Chem.*, 2011, **21**, 3779–3787.
22 B. Mallik, K. M. Jain and T. N. Misra, *Biochem. J.*, 1980, **189**, 547–552.
23 M. Khaled, A. Hadjipetrou, L. D. Kispert and R. D. Allendoerfer, *J. Phys. Chem.*, 1991, **95**, 2438–2442.
24 T. W. Ebbesen, R. Akaba, K. Tokumaru, M. Washio, S. Tagawa and Y. Tabatal, *J. Am. Chem. Soc.*, 1988, **110**, 2147–2151.
25 J. A. Jeevarajan, C. C. Wei, A. S. Jeevarajan and L. D. Kispert, *J. Phys. Chem.*, 1996, **100**, 5637–5641.
26 J. H. Lee, B. Ozcelik and D. B. Min, *J. Food Sci.*, 2003, **68**, 861–865.
27 K. Yanagi, Y. Miyata and H. Kataura, *Adv. Mater.*, 2006, **18**, 437–441.
28 J. S. Hu, L. L. Ren, Y. G. Guo, H. P. Liang, A. M. Cao, L. J. Wan and C. L. Bai, *Angew. Chem., Int. Ed.*, 2005, **44**, 1269–1273.
29 A. Mandal, A. Dandapat and G. De, *Analyst*, 2012, **137**, 765–772.
30 N. Guijarro, J. M. Campin, Q. Shen, T. Toyoda, T. L. Villarreal and R. Gomez, *Phys. Chem. Chem. Phys.*, 2011, **13**, 12024–12032.
31 W. G. Becker and A. J. Bard, *J. Phys. Chem.*, 1983, **87**, 4888–4893.
32 H. R. Shakur, *Phys. E.*, 2011, **44**, 641–646.
33 K. Dimos, I. B. Koutselas and M. A. Karakassides, *J. Phys. Chem. B*, 2006, **110**, 22339–22345.
34 J. H. Yu, J. Joo, H. M. Park, S.-II. Baik, Y. W. Kim, S. C. Kim and T. Hyeon, *J. Am. Chem. Soc.*, 2005, **127**, 5662–5670.
35 S. Sapra, A. Prakash, A. Ghangrekar, N. Periasamy and D. D. Sarma, *J. Phys. Chem. B*, 2005, **109**, 1663–1668.
36 M. Mall and L. Kumar, *J. Lumin.*, 2010, **130**, 660–665.
37 P. Yang, M. Lu, D. Xu, D. Yuan and G. Zhou, *Appl. Phys. A: Mater. Sci. Process.*, 2001, **73**, 455–458.
38 D. B. Cullity, *Elements of X-Ray Diffraction*, Addison-Wesley Publishing Company, UK, 1978, Ed. 2, CH. 9, p. 284, (ISBN-13: 9780201011746).
39 V. E. De-Oliveira, H. V. Castro, H. G. M. Edwards and L. F. C. De-Oliveira, *J. Raman Spectrosc.*, 2010, **41**, 642–650.
40 T. Takenobu, T. Takano, M. Shiraishi, Y. Murakami, M. Ata, H. Kataura, Y. Achiba and Y. Iwasa, *Nat. Mater.*, 2003, **2**, 683–688.
41 C. N. R. Rao, A. K. Sood, K. S. Subrahmanyam and A. Govindaraj, *Angew. Chem., Int. Ed.*, 2009, **48**, 7752–7777.
42 S. Wageh, Z. S. Ling and X. X. Rong, *J. Cryst. Growth*, 2003, **255**, 332–337.
43 L. W. Yin, Y. Bando, J. H. Zhan, M. S. Li and D. Golberg, *Adv. Mater.*, 2005, **17**, 1972–1977.
44 J. Hu, Y. Bando, J. Zhan and D. Golberg, *Adv. Funct. Mater.*, 2005, **15**, 757–762.
45 S. L. Bondarev and V. N. Knyukshto, *Chem. Phys. Lett.*, 1994, **225**, 346–350.
46 J. A. Kloepfer, N. Cohen and J. L. Nadeau, *J. Phys. Chem. B*, 2004, **108**, 17042–17049.
47 I. L. Medintz, L. Berti, T. Pons, A. F. Grimes, D. S. English, A. Alessandrini, P. Facci and H. Mattoussi, *Nano Lett.*, 2007, **7**, 1741–1748.
48 M. Sharma, S. Singh and O. P. Pandey, *J. Appl. Phys.*, 2010, **107**, 104319.
49 G. Gao, Y. Deng and L. D. Kispert, *J. Phys. Chem. B*, 1998, **102**, 3897–3901.
50 H. Hashimoto and Y. Koyama, *J. Phys. Chem.*, 1988, **92**, 2101–2108.
51 B. Robert, *The Photochemistry of Carotenoids*, ed. H. A. Frank, A. J. Young, G. Britton and R. J. Cogdell, Springer-Kluwer Academic Publishers, The Netherlands, USA, 1999, vol. 8, p. 420, (ISBN: 0-7923-5942-9).
52 T. Noguchi, T. Mitsuka and Y. Inoue, *FEBS Lett.*, 1994, **356**, 179–182.
53 M. T. Liu, W. T. Cheng, M. J. Li, H. N. Liu, D. M. Yang and S. Y. Lin, *Arch. Dermatol. Res.*, 2005, **297**, 231–234.
54 M. J. Bowers II, J. R. McBride and S. J. Rosenthal, *J. Am. Chem. Soc.*, 2005, **127**, 15378–15379.
55 S. Sapra, S. Mayilo, T. A. Klar, A. L. Rogach and J. Feldmann, *Adv. Mater.*, 2007, **19**, 569–572.
56 C. C. Shen and W. L. Tseng, *Inorg. Chem.*, 2009, **48**, 8689–8694.